NASA Technical Memorandum 83491

NASA-TM-83491 19830027141

The Structural Response of a Rail Accelerator

S. Y. Wang
Lewis Research Center
Cleveland, Ohio

Prepared for the
Second Symposium on Electromagnetic Launch Technology
sponsored by the Institute of Electrical and Electronics Engineers
Boston, Massachusetts, October 10–14, 1983

NASA

THE STRUCTURAL RESPONSE OF A RAIL ACCELERATOR

S. Y. Wang

National Aeronautics and Space Administration
Lewis Research Center
Cleveland, Ohio 44135

Abstract

The transient response of a 0.4 by 0.6 cm rectangular bore rail accelerator was analyzed using a three-dimensional finite-element code. Results are presented for the case of a 210-kA current input and 5-cm arc length. Typically, the copper rail deflected to a peak value of 0.08 mm in compression and then oscillated at an amplitude of 0.02 mm. Simultaneously the insulating side wall of glass fabric base, epoxy resin laminate (G-10) was compressed to a peak value of 0.13 mm and rebounded to a steady state in extension. Projectile pinch or blow-by due to the rail (or side-wall) extension or compression, respectively, can be identified by examining the time history of the rail (or side-wall) displacement. For the case presented, the effect of blow-by was most significant at the side wall characterized by mm-size displacement in compression.

Dynamic stress calculations indicate that the G-10 supporting material behind the rail is subjected to over 21 MPa – at which the G-10 could fail if the laminate was not carefully oriented. Results for a polycarbonate resin (Lexan) side wall show much larger displacements and stresses than for G-10. Therefore the tradeoff between the transparency of Lexan and the mechanical strength of G-10 for side-wall material is obvious.

Displacement calculations from the modal method are smaller than the results from the direct integration method by almost an order of magnitude, because the high-frequency effect is neglected. However, this effect is significant and dominating for a highly-impulsive, wave-propagation problem such as the rail accelerator structure.

Introduction

A rail accelerator imparts high velocity to a projectile through the application of large impulsive forces of short duration. For the case of a plasma armature, the rail accelerator structure is dynamically stressed by the plasma pressure and magnetic forces immediately behind the projectile. [1] The impulsive loading causes stress waves to propagate through the structure inducing responses in the materials at the wave speed. Displacements of the rails and insulating side walls ahead of the projectile may hinder the performance of the accelerator [2] due to a combination of two effects: pinch and blow-by. The former occurs when the rails or side walls pinch into the projectile and frictional interaction intensifies; the latter occurs when the clearance between the projectile and the rails or side walls opens allowing the plasma to blow by the projectile. These effects can be detrimental if the design of the rail and supporting structures are insufficient to handle the intensive pulse loading of hundreds of megapascals.

Numerical analysis can be used to estimate the structural response of the rail accelerators. For some rail geometries, one or two-dimensional analyses [3,4] have been applied to estimate the maximum rail deflections and the relative effects of different structural or material properties. However, it is desirable to use a three-dimensional transient program to model a rail accelerator structure to visualize the transient deflections of the rail in three dimensions as well as the propagation of the stress wave.

The primary purpose of this paper is to predict the transient rail and side-wall displacements of a 0.4 cm by 0.6 cm rectangular bore, one meter long rail accelerator using the three-dimensional finite-element code MARC on CRAY/IBM computers. Both rail and side wall deflections are estimated by applying a pulsed plasma loading on both the side wall and the rail and a magnetic loading on the rail behind the projectile. A secondary purpose is to calculate the stress of the supporting materials, including a glass fabric base, epoxy resin laminate (G-10), a polycarbonate resin (Lexan), and a phenolic resin.

Results are presented using the Newmark direct integration method for a typical case of 210-kA current input, with a 5-cm plasma arc length at an instantaneous velocity of 2.5 km/s. A modal method using 10 modes is also used for comparison.

Analytical Procedures

When a material is subjected to a significant dynamic loading, disturbances are propagated through the body as stress waves. Deformations resulting from the impulsive loading will be highly localized within the region influenced by the stress wave, while the global structure effect is small. For this case wide-spectrum frequencies are excited; however, the high-frequency modes usually dominate throughout the time of interest. [5]

Finite-element Code

The three-dimensional finite-element computer code, MARC [6], is available in both modal method and direct integrating method. The former allows a choice of 10 modes and is generally good for low-frequency structural dynamic problems. The latter is appropriate for high-loading, wave-propagation problems such as the rail accelerator. The direct Newmark integration method was selected for the analysis, and the 10-mode modal method was used for comparison purposes.

The finite element mesh plot was generated and shown in Fig. 1(a). Only a quadrant of the rail accelerator, of Figs. 1(b) and (c), is needed because of two planes of symmetry. The element used is a 8-node, isoparametric, three-dimensional hexahedron block. The mesh model consists of 300 elements and 504 nodes. A typical run on the CRAY-1S uses about 18 minutes (in CPU). All the outputs and post plots are then transferred to a front computer the IBM 3033.

For the cases studied, the materials used for the rail accelerator were held within the elastic limits. Any plastic distortion or non-linear effect is undesirable. Furthermore, the secondary effect of damping is not included in this report which represent the upper bound values of both displacement and stress.

Input Conditions

A rail accelerator one meter long with a bore of 0.4 by 0.6 cm was simulated. Rails are made of copper, and side-wall and supporting structures are made of G-10/Lexan and phenolic resin. Their properties are

listed in Table I. A high current plasma armature was produced to accelerate the projectile between the rails.

Referring to Fig. 1, the projectile is set to a starting position (reference nodal point 2) and is accelerated by the arc plasma covering bore walls of element numbers 1 and 241 along the x-direction between the rail, all the way through to the muzzle end (reference nodal point 21).

Loading Conditions

Loading inputs include both arc plasma pressure (P_p) and rail magnetic pressure (P_r). P_p is acting on the back of the projectile of an area (A_p) and is propotional to the Lorentz force (F_p). F_p is obtained from the input current (I) and the inductance gradient (L') of the rail:

$$P_p = \frac{F_p}{A_p} = \frac{L'I^2}{2\,h_p\,S}$$

where h_p is the rail height, and s is the distance between the rails. P_r is equal to the magnetic force (F_r) per unit rail area (A_r) and is acting on the rail only:

$$P_r = \frac{F_r}{A_r} = \frac{I^2}{2\,h_p\,h} \cdot \frac{dL'}{d(S/h)}$$

where h is the arc plasma height, and $dL'/d(S/h)$ is the inductance gradient calculated for this geometry. [7]

It is assumed that P_p is uniformly distributed behind the projectile within an arc length (L_a). The acting period of time (Δt) of P_p on a specific element wall is then L_a/V_m; where V_m is the instantaneous speed of the arc traveling through the bore, and L_a can be estimated by combining available measured values [8,9] and the scaling laws. [10]

Typical values used for the calculations are listed in Table II.

For illustration, the transient pressure inputs are plotted in Fig. 2 for rail elements 1 through 4, and also for side-wall elements 241 through 244. Where a flat-topped pulse of 20 μsec is assumed for P_p of 450 MPa and a constant P_r is 240 MPa. With known arc length and speed, only the arc shape is assumed for the transient loading inputs.

Different pulse shapes of inertia loading and responses have been well investigated. [11] The square wave renders the maximum response, by an amplification factor of two, as compared to other shapes: sinusoidal, triangular, sudden-rise, or sudden-fall. The flat-topped shape pulse assumed in the paper should give more conservative values of displacement, although the actual shape of loading may be quite complicated.

Results and Discussions

The primary case (P41) is calculated using G-10 as the side-wall insulator and applying the direct integration method. Two secondary cases are included for the relative comparison of using transparent Lexan as the side-wall material (Case N41) and of applying the modal method with ten modes (Case Q41).

The Primary Case (P41)

Time history results are presented for both rail and side-wall displacements, the element stress of G-10 backing material behind the rail, and the sectional stress contours of case P41.

Figure 3 shows the rail displacements at the breech end (nodes 1 and 2) and the muzzle end (nodes 20 and 21). Each nodal point has a similar response characterized by a pulse due to the impulsive loading and then approaching a quasi-steady value. Figure 4 shows that the typical response of a single node 3, 5-cm downstream of the projectile's starting position which is another 5 cm from the breech end. It also shows the peak displacement reaches 0.06 mm of compression and oscillates, with a period of 30 μsec within 0.01 to 0.03 mm range. The instantaneous position of the projectile corresponds to a 40 μsec time scale in Fig. 4, where a compression of 0.03 mm indicates possible blow-by which means the plasma leaks through the clearance to the front of the projectile. The actual processes of blow-by or pinch are complicated because of their high-speed, high-temperature, and dynamic features. However the transient displacement can be used as a critical parameter to assess the possibility of blow-by or pinch. Criterion for the parameter may be different for different accelerators under various operating conditions.

Corresponding side-wall displacements are plotted in Fig. 5, at the breech end (nodes 421 and 422) and at the muzzle end (nodes 440 and 441). Peak deflections of between 0.07-0.15 mm are obtained along the one meter length of the accelerator, while the quasi-steady deflections are under extension (indicated by minus values). Figure 6 shows the displacements of node 423. At the current projectile position 5-cm downstream (corresponding to 40 μsec), a compression of 0.07 mm indicates that the effect of blow-by may be larger than that on the rail. However, the pinch effect seems to be negligible on the projectile because the displacements are mostly positive at that instant.

The transient stress calculation for G-10 element 83 (which is under element 23 in Fig. 1(a)) exhibits a typical variation during the time of interest as shown in Fig. 7. This element behind the rail, at 5-cm downstream of the projectile's starting position, has a stress wave form similar to these of displacement response, peaked at 22 MPa and approached quasi-steady value of 8 MPa. If the G-10 laminates are oriented in the weakest direction at which the yield strength is approximately 7 MPa, failure can occur. [12] Stress contours are plotted at a section cut through the rail and its G-10 backing material (elements 61 through 100 and 241 through 260), for each 100 μsec time period. The traveling characteristic of the stress wave can be seen from Fig. 8 where the stress concentration reaches 410 MPa on the rail for most of the time while peaked at 700 MPa at the end due to rebounding at the muzzle end.

Secondary Case (N41)

It can be seen from Fig. 9 that the deflection reaches 0.8 mm using Lexan as the side-wall material. This displacement is about an order of magnitude larger than the G-10 case shown in Fig. 6, and the effect of blow-by will be significant. The use of Lexan at high current (210-kA) seems to be unfeasible. The trade off between the transparency and the operating current, or the mechanical strength, is thus obvious.

Secondary Case (Q41)

For the purpose of demonstrating the difference between the application of numerical methods, the same input conditions of the primary case is calculated by using the modal method. As shown in Fig. 10, rail

displacements are much smaller. On the other hand periods are larger when compared with Fig. 4. The reason for these differences is the modal method does not include enough modes so that the dominating effects of high frequencies of the wave are neglected. On the other hand, the direct integration method is appropriate for the highly impulsive, wave-propagation problem such as the rail accelerator.

Concluding Remarks

The response of a rail accelerator structure to an impulsive loading can be predicted by a three-dimensional, finite-element code - MARC using the direct integration method. The effects of blow-by or pinch are shown by rail or side-wall displacements. Mechanical limits are also discussed to the first order by calculating the dynamic stress values. Relative merits of different materials or geometry can readily be assessed.

References

1. E.E. Rice, L.A. Miller, and R.W. Earhart, "Preliminary Feasibility Assessment for Earth-to-Space Electromagnetic (Railgun) Launchers," NASA CR-167886, Battelle Columbus Lab., June 30, 1982.

2. D.R. Peterson, et al., Monthly Letter, Los Alamos National Lab., Feb. 12, 1982.

3. R.F. Davidson, Los Alamos National Lab., Private Communication, Dec. 1982.

4. R.S. Hawke, and J.K. Scudder, "Magnetic Propulsion Railguns: Their Design and Capabilities", UCRL-82677, Lawrence Livermore Lab., 1979.

5. J.A. Zukas, et al., Impact Dynamics, John Wiley a Sons, Inc. 1982.

6. "MARC General Purpose Finite Element Program," User Manual Vol. A-E, MARC Analysis Research Corp. Palo Alto, CA., 1982.

7. J.F. Kerrisk, "Current Distribution and Inductance Calculations for Rail-Gun Conductors," LA-9092-MS Los Alamos National Lab., Nov. 1981.

8. J.V. Parker, D.R. Peterson, C.E. Cummings, and C.M. Fowler, "Measurement of Railgun Arc Characteristics," LA-UR82-2177, Los Alamos National Lab., Nov. 1982.

9. K.A. Jamison, and H.S. Burden, "Arc Armature Diagnostic Experiments On An Electromagnetic Gun," ARRADCOM Technical Conference Paper, Ballistic Research Lab., July 1982.

10. J.D. Powell and J.H. Batteh, "Plasma dynamics of an arc-driven, electromagnetic, projectile accelerator," Ballistic Research Lab., J. Appl. Phys., Vol. 52, pp. 2717-2730, April 1981.

11. M. Kornhauser, Structural Effect of Impact. Baltimore: Spartan Books, 1964.

12. D.P. Bauer, T.J. McCormick, and J.P. Barber, "Electric Rail Launcher System Design and Test Evaluation," IAP-TR-82-6. IAP Research, Inc. Nov. 1982.

TABLE I. - PROPERTIES OF RAIL ACCELERATOR MATERIALS

	Young's modulus, GPa	Poisson ratio	Density, gm/cm^3	Yield point, MPa
Copper	117	0.37	8.4	400
G-10 Laminate	17.2	0.33	1.75	7-350*
Lexan	2.3	0.33	1.2	63
Phenolic Resin	8.3	0.33	1.4	45

*Depends on orientation of the laminates.

TABLE II. - VALUES USED FOR CALCULATIONS

Current I, KA	Arc length, L_a, cm	Velocity V_m, km/s	Inductance gradient L', μh/m	Inductance gradient dL'/d(S/h), μh/m	Rail height h, cm	Arc height h_p cm	Rail width s, cm
210	5	2.5	0.48	0.245	0.63	0.38	0.63

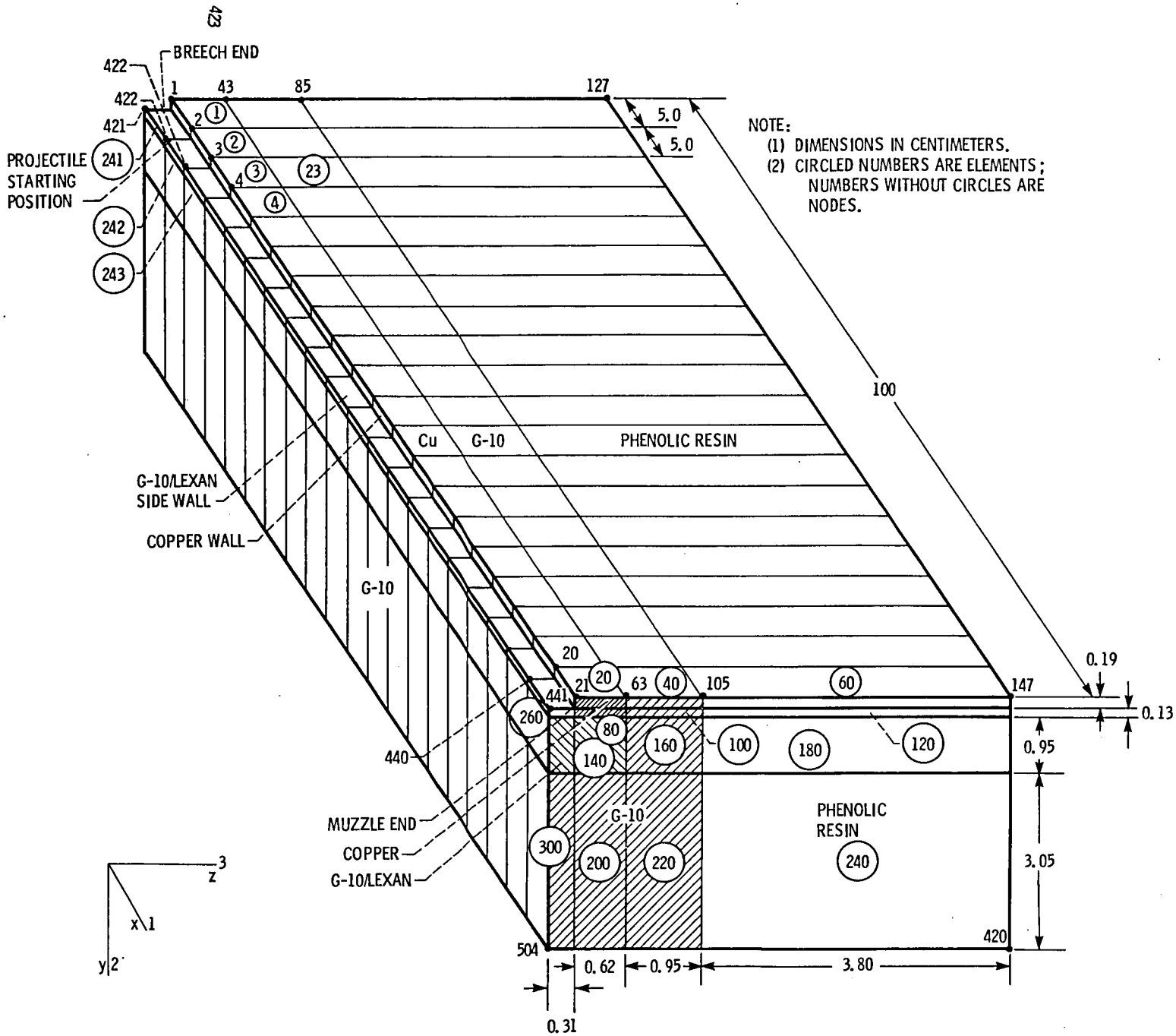

(a) Mesh plot of the 0.4x0.6 cm rail accelerator.

Figure 1.

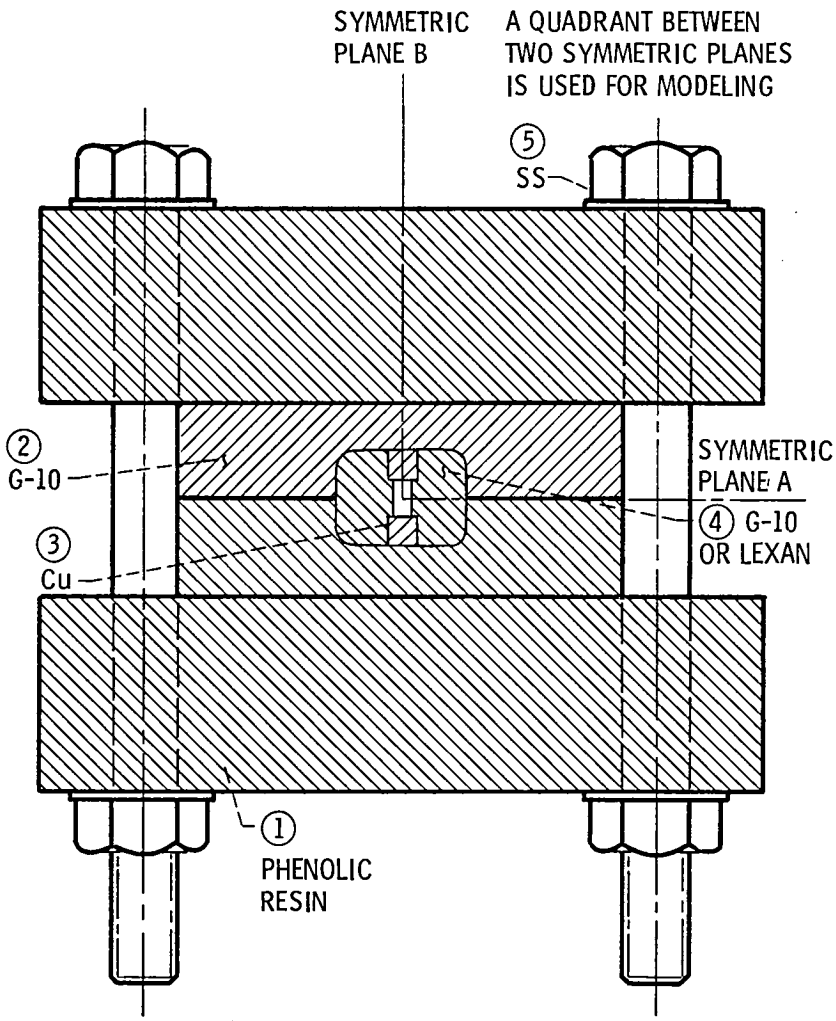

(b) Rail accelerator cross section.

Figure 1. - Continued.

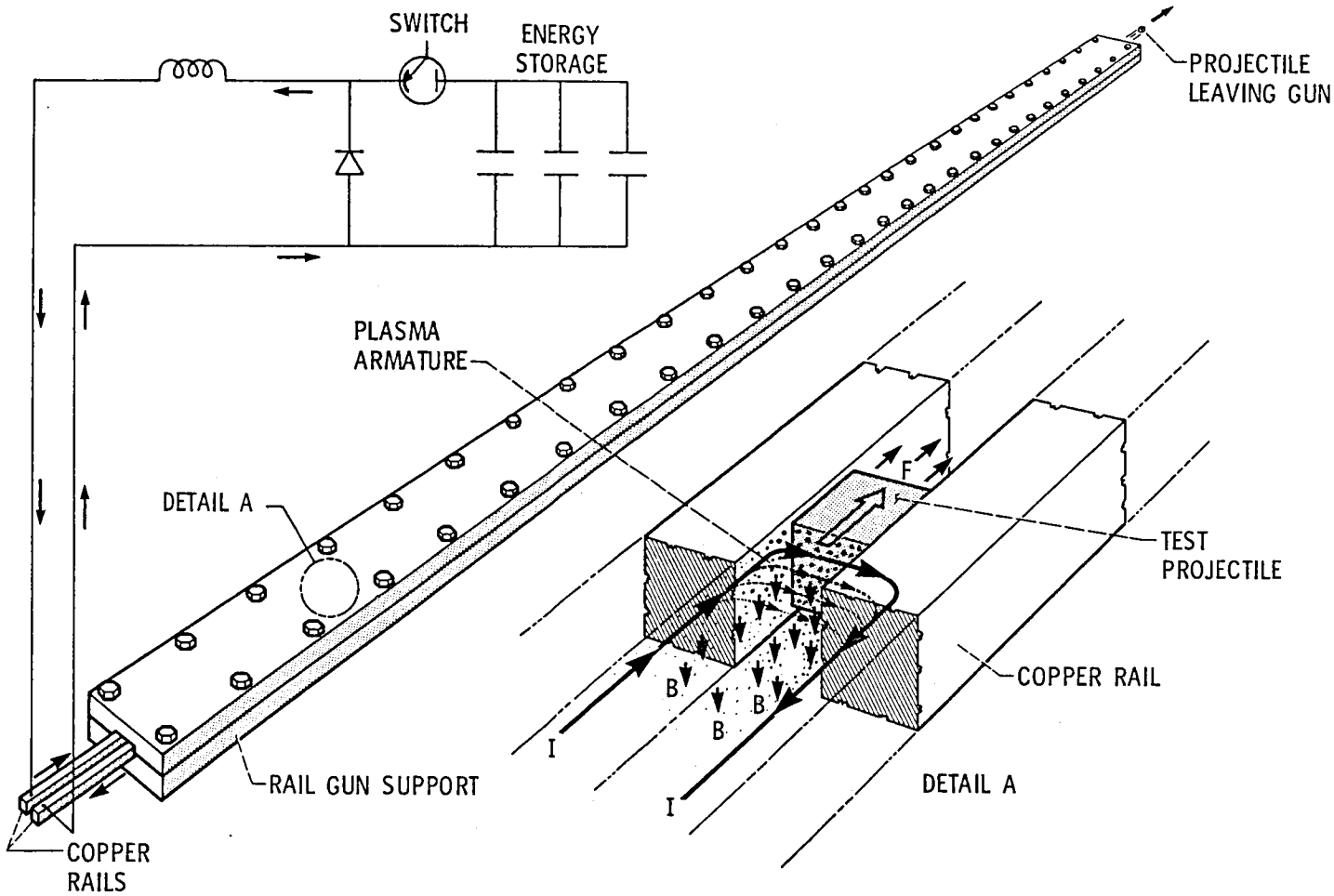

(c) Rail accelerator (gun).

Figure 1. - Concluded.

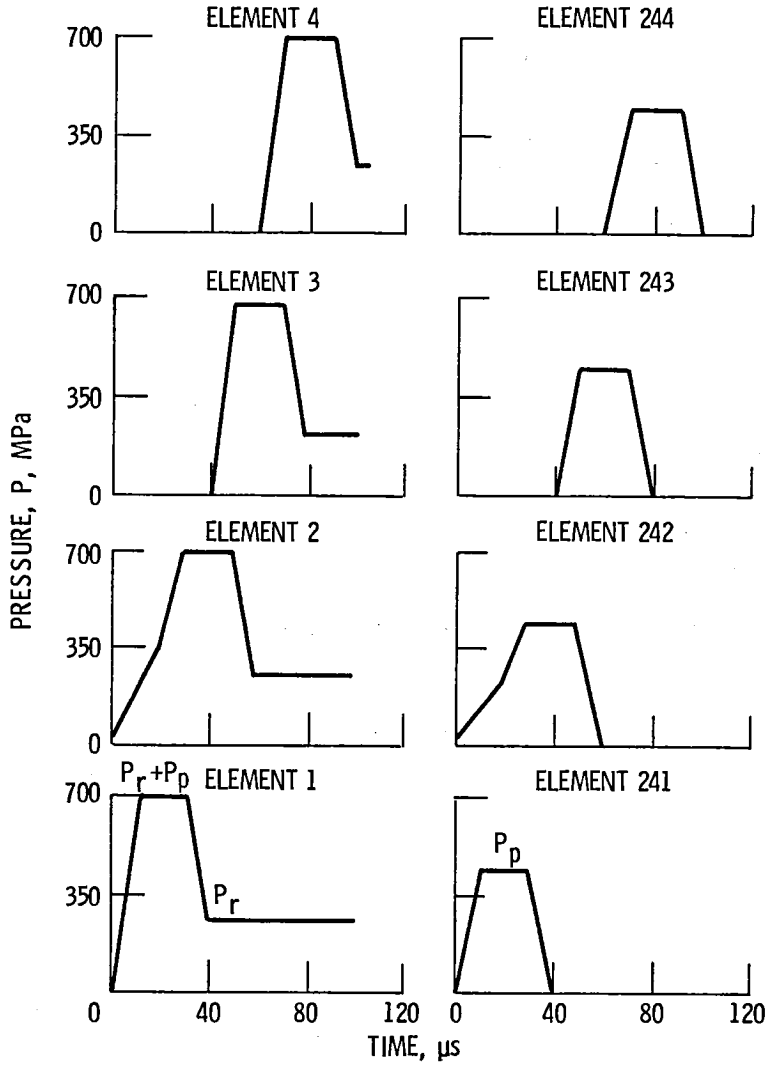

Figure 2. - Transient profiles of pressure loading for the first four elements of both the rail (1-4) and side wall (241-244).

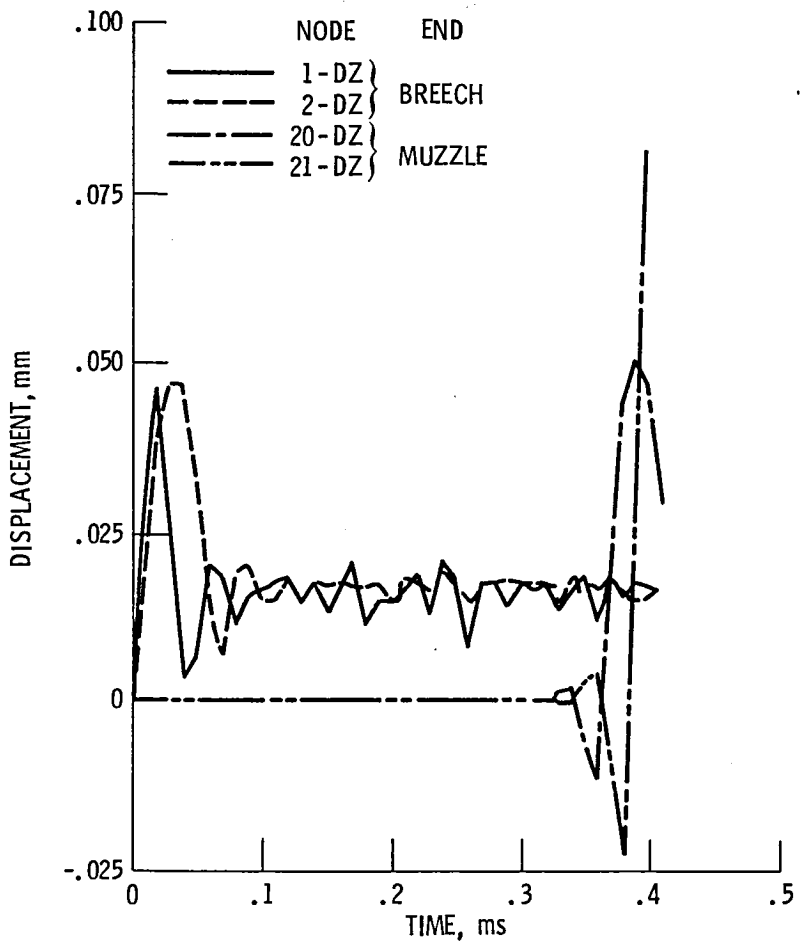

Figure 3. - Rail displacements at breech and muzzle ends.

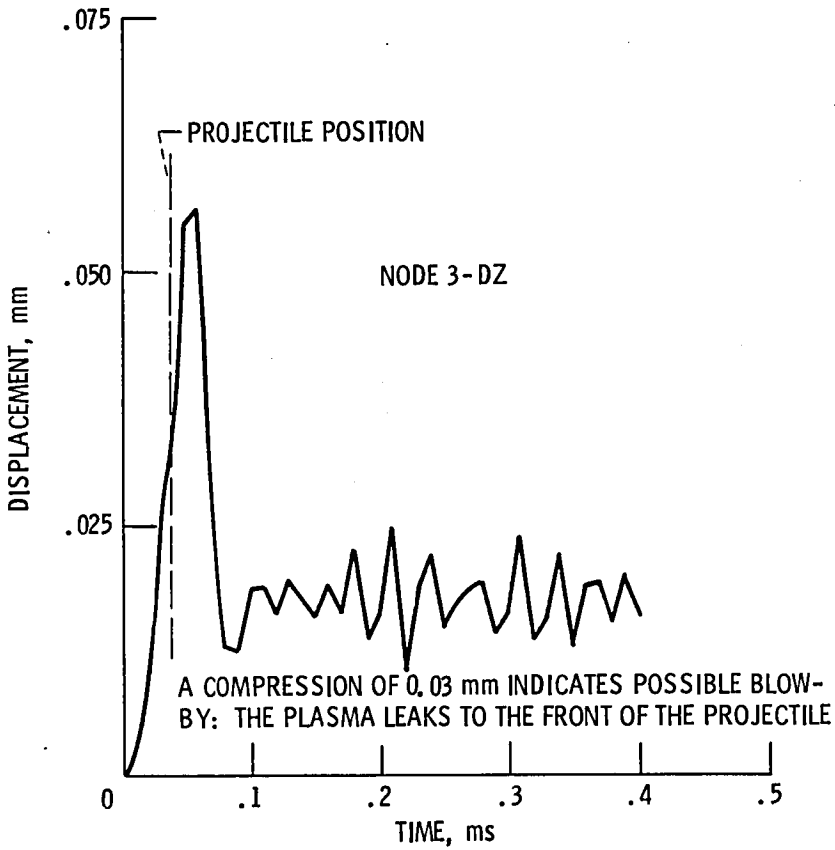

Figure 4. - Rail displacement 5-cm downstream.

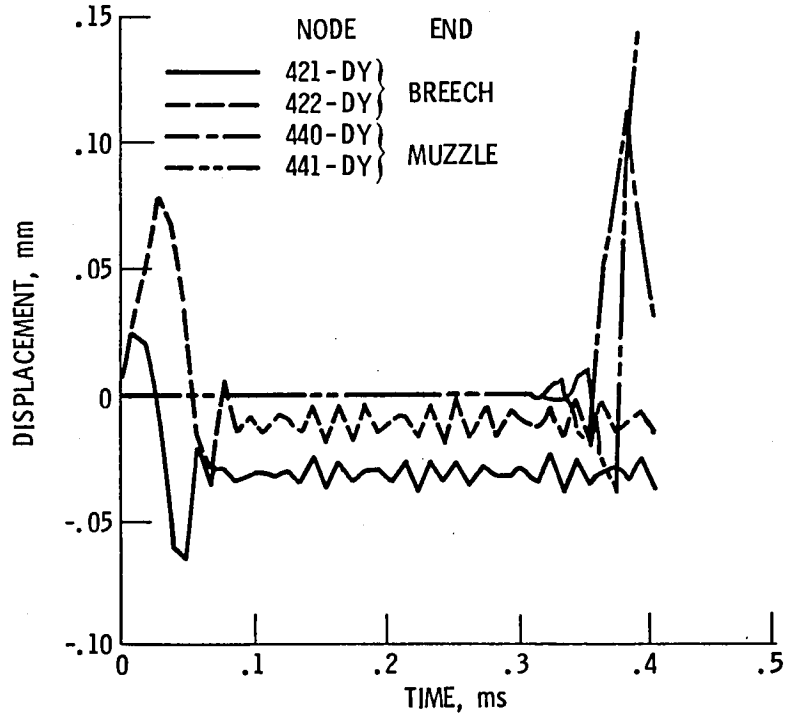

Figure 5. - Side-wall displacements at breech/muzzle ends.

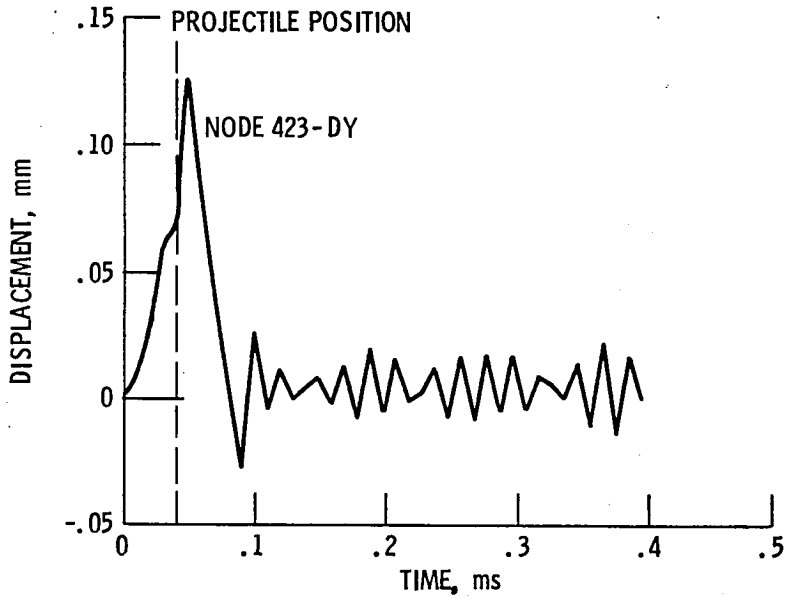

Figure 6. - Side-wall G-10 displacement 5-cm downstream.

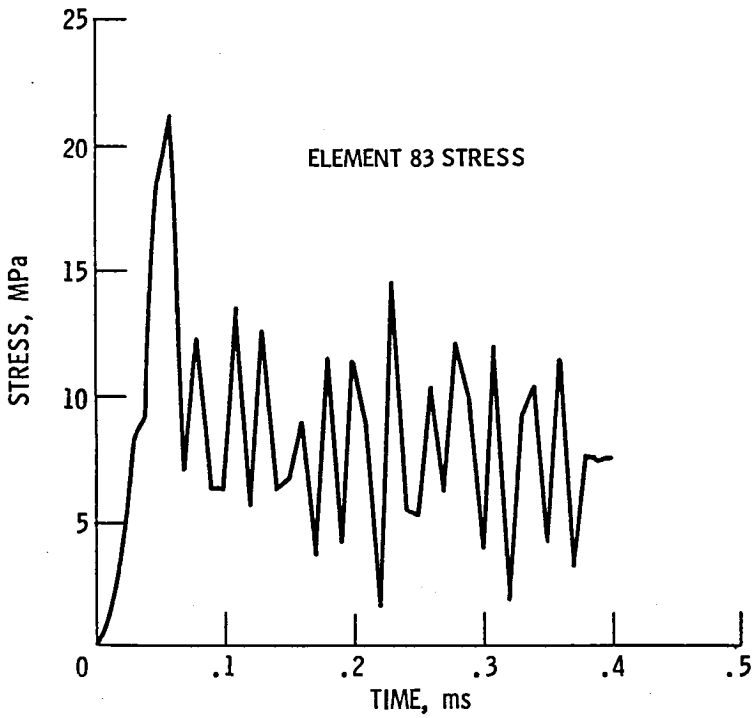

Figure 7. - Stress in G-10 backing material 5-cm downstream.

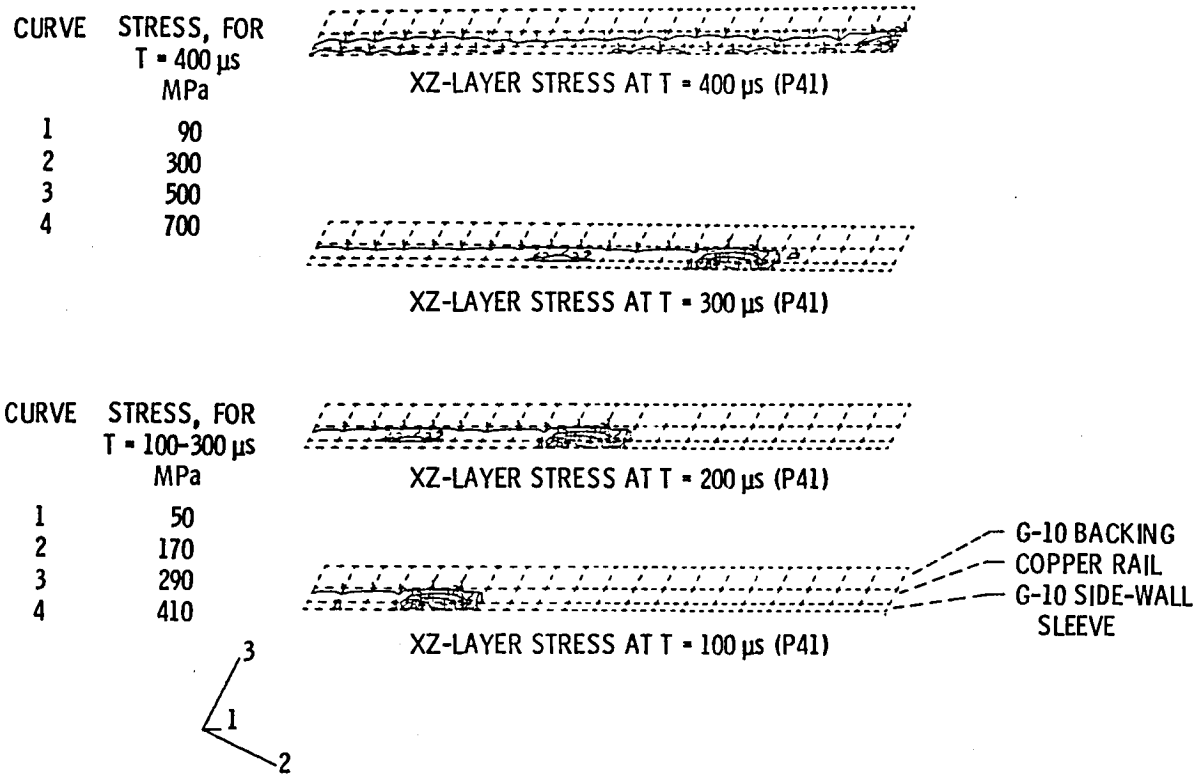

Figure 8. - Transient stress contours for copper rail (elements 61-80), G-10 backing (elements 81-100), and G-10 siding (elements 241-260).

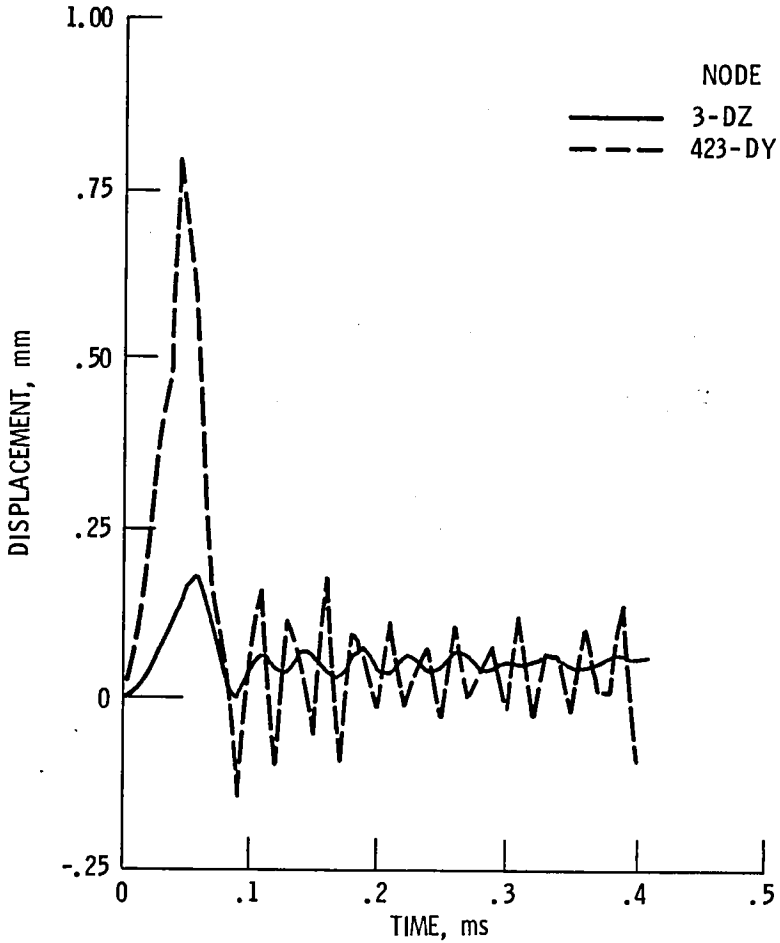

Figure 9. - Displacements 5-cm downstream using lexan.

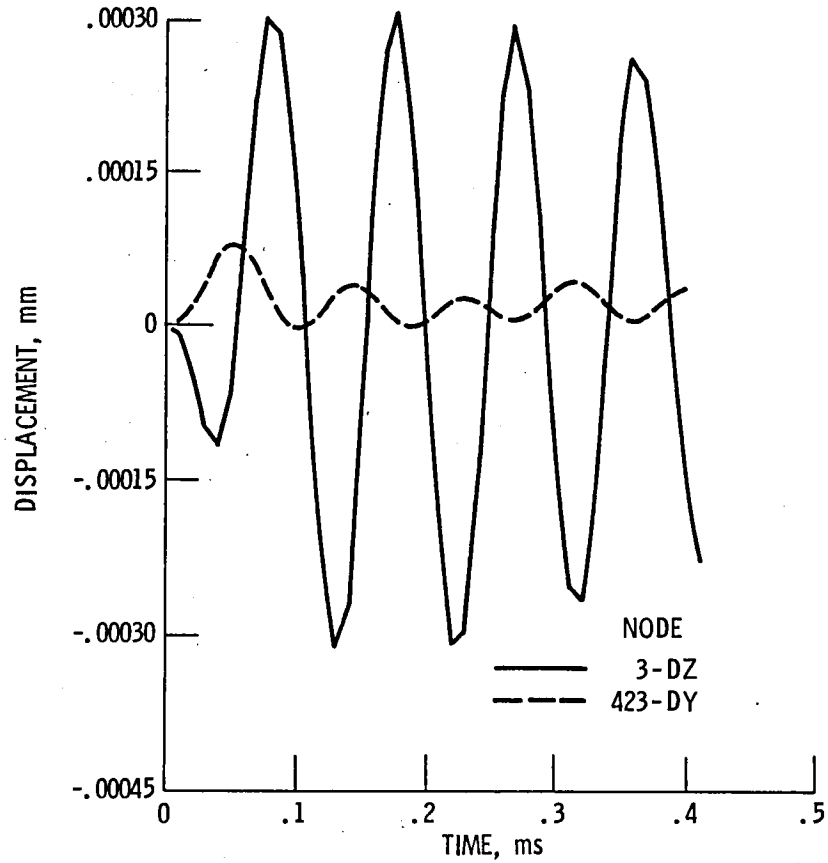

Figure 10. - Displacements 5-cm downstream modal method.

1. Report No.	2. Government Accession No.	3. Recipient's Catalog No.
NASA TM-83491		

4. Title and Subtitle	5. Report Date
The Structural Response of a Rail Accelerator	6. Performing Organization Code: 506-55-22
7. Author(s): S. Y. Wang	8. Performing Organization Report No.: E-1820
	10. Work Unit No.
9. Performing Organization Name and Address: National Aeronautics and Space Administration, Lewis Research Center, Cleveland, Ohio 44135	11. Contract or Grant No.
12. Sponsoring Agency Name and Address: National Aeronautics and Space Administration, Washington, D.C. 20546	13. Type of Report and Period Covered: Technical Memorandum
	14. Sponsoring Agency Code

15. Supplementary Notes

Prepared for the Second Symposium on Electromagnetic Launch Technology, sponsored by the Institute of Electrical and Electronics Engineers, Boston, Massachusetts, October 10-14, 1983.

16. Abstract

The transient response of a 0.4 by 0.6 cm rectangular bore rail accelerator was analyzed using a three-dimensional finite-element code. Results are presented for the case of a 210-kA current input and 5-cm arc length. Typically, the copper rail deflected to a peak value of 0.08 mm in compression and then oscillated at an amplitude of 0.02 mm. Simultaneously the insulating side wall of glass fabric base, epoxy resin laminate (G-10) was compressed to a peak value of 0.13 mm and rebounded to a steady state in extension. Projectile pinch or blow-by due to the rail (or side-wall) extension or compression, respectively, can be identified by examining the time history of the rail (or side-wall) displacement. For the case presented, the effect of blow-by was most significant at the side wall characterized by mm-size displacement in compression. Dynamic stress calculations indicate that the G-10 supporting material behind the rail is subjected to over 21 MPa - at which the G-10 could fail if the laminate was not carefully oriented. Results for a polycarbonate resin (Lexan) side wall show much larger displacements and stresses than for G-10. Therefore the tradeoff between the transparency of Lexan and the mechanical strength of G-10 for side-wall material is obvious. Displacement calculations from the modal method are smaller than the results from the direct integration method by almost an order of magnitude, because the high-frequency effect is neglected. However, this effect is significant and dominating for a highly-impulsive, wave-propagation problem such as the rail accelerator structure.

17. Key Words (Suggested by Author(s))	18. Distribution Statement
Propulsion Rail gun Structure dynamics	Unclassified - unlimited STAR Category 39

19. Security Classif. (of this report)	20. Security Classif. (of this page)	21. No. of pages	22. Price*
Unclassified	Unclassified		

*For sale by the National Technical Information Service, Springfield, Virginia 22161

National Aeronautics and
Space Administration

Washington, D.C.
20546

Official Business
Penalty for Private Use, $300

SPECIAL FOURTH CLASS MAIL
BOOK

U.S.MAIL

Postage and Fees Paid
National Aeronautics and
Space Administration
NASA-451

NASA

POSTMASTER: If Undeliverable (Section 158
Postal Manual) Do Not Return